

ARTICLE OPEN



Rapid transformation of wildfire emissions to harmful background aerosol

Christina N. Vasilakopoulou^{1,2}, Angeliki Matrali^{1,2}, Ksakousti Skyllakou², Maria Georgopoulou^{1,2}, Andreas Aktypis^{1,2}, Kalliopi Florou², Christos Kaltsonoudis², Evangelia Siouti^{1,2}, Evangelia Kostenidou³, Agata Błaziak⁴, Athanasios Nenes^{2,5}, Stefanos Papagiannis⁶, Konstantinos Eleftheriadis⁶, David Patoulias⁷, Ioannis Kioutsoukis⁷ and Spyros N. Pandis^{1,2}✉

Wildfires are a significant source of organic aerosol during summer, with major impacts on air quality and climate. However, studies in Europe suggest a surprisingly low (less than 10%) contribution of biomass burning organic aerosol to average summertime fine particulate matter levels. In this study we combine field measurements and atmospheric chemical transport modeling, to demonstrate that the contribution of wildfires to fine particle levels in Europe during summer is seriously underestimated. Our work suggests that the corresponding contribution has been underestimated by a factor of 4–7 and that wildfires were responsible for approximately half of the total OA in Europe during July 2022. This discrepancy with previous work is due to the rapid physicochemical transformation of these emissions to secondary oxidized organic aerosol with an accompanying loss of its organic chemical fingerprints. These atmospheric reactions lead to a regionally distributed background organic aerosol that is responsible for a significant fraction of the health-related impacts caused by fine particles in Europe and probably in other continents. These adverse health effects can occur hundreds or even thousands of kilometers away from the fires. We estimate that wildfire emissions are responsible for 15–22% of the deaths in Europe due to exposure to fine particulate matter during summer.

npj Climate and Atmospheric Science (2023)6:218; <https://doi.org/10.1038/s41612-023-00544-7>

INTRODUCTION

Biomass burning organic aerosol (OA) is one of the major pollutants emitted by wildfires¹. Every year millions of significant wildfires occur all around the globe. Bottom-up estimates of wildfire emissions suggest that they are responsible for more than 85% of the fine particulate matter emissions in Europe during summer² and therefore they are a major contributor to air quality deterioration and the corresponding health effects on humans. On the other hand, top-down estimates based on measurements³ of the composition of the PM₁ suggest that they are responsible for less than 10% of the OA. This major discrepancy results in significant uncertainty about the current role of wildfires as an air pollution source especially far from the corresponding fire areas.

Measurements were conducted in a remote continental eastern Mediterranean site (Pertouli, Greece) in the summer of 2022, in order to quantify the impact of wildfires on the air quality in this region (SPRUCE-22 campaign). Several wildfires occurred across Europe during the study period³, producing on average 38,000 tn d⁻¹ of PM_{2.5}. Fires in the Iberian Peninsula were responsible for 30% of these emissions (Supplementary Fig. 1). Major fires also occurred in Ukraine. The wildfire emissions during July 2022 in Europe were relatively high in the Iberian Peninsula and the rest of Western Europe, but normal for a summer month in the rest of the continent. There were no fires within 100 km of the site and relatively few fires in Greece in general. The anthropogenic organic PM_{2.5} emissions during the study period were estimated at 4700 tn d⁻¹, less than one quarter of the biomass burning emissions⁴.

Source apportionment of the measured OA in Pertouli was conducted using Positive Matrix Factorization of the Aerosol Mass

Spectrometer measurements^{5,6}. Despite the occurrence of all these fires in Europe, the source apportionment analysis was unable to identify biomass burning (bbOA) as a significant OA source. On the contrary, three secondary factors were identified: biogenic-oxidized OA (bOOA) (23% of the total OA), less-oxidized OA (LO-OOA) (37% of OA) and more-oxidized OA (MO-OOA) (40% of OA) (Fig. 1) raising the question of what happened to the bbOA. The ME-2 algorithm was used to estimate a potential upper bound of the concentration of fresh bbOA⁷ forcing the solution to include a fresh bbOA factor⁸. Even in this case, the average bbOA was only 3% of the total OA (0.2 μg m⁻³) for the examined period (Supplementary Fig. 2). The OA in the site was highly oxidized (O:C = 0.85).

Our hypothesis is that the biomass burning emissions react rapidly in the atmosphere and are transformed to oxidized OA. The transformations include evaporation of the semi-volatile bbOA components, reactions in the gas phase and then recondensation of the products of the oxidation, heterogeneous reactions of the primary biomass burning with OH and reactions in the aqueous phase (both in clouds and during periods of high RH)^{9,10}. This chemical aging of bbOA leads to rapid loss of its organic chemical fingerprints (e.g., levoglucosan), thus resulting in a serious underestimation of its contribution to the OA levels. The high summertime temperature, sunlight intensity and high oxidant levels accelerate the corresponding processes. If this hypothesis is valid, the importance of biomass burning during summer is currently seriously underestimated and is a lot more than 8% of the OA. It may contribute to a large extent to the European background OA during summer to which all Europeans are exposed.

¹Department of Chemical Engineering, University of Patras, Patras, Greece. ²Institute of Chemical Engineering Sciences, ICE-HT, Patras, Greece. ³Department of Environmental Engineering, Democritus University of Thrace, Xanthi, Greece. ⁴Institute of Physical Chemistry, Polish Academy of Sciences, 01-224 Warsaw, Poland. ⁵School of Architecture, Civil and Environmental Engineering, Ecole Polytechnique Fédérale de Lausanne, Lausanne 1015, Switzerland. ⁶ERL, Institute of Nuclear & Radiological Sciences & Technology, Energy & Safety, National Centre of Scientific Research Demokritos, Athens, Greece. ⁷Department of Physics, University of Patras, Patras, Greece. ✉email: spyros@chemeng.upatras.gr

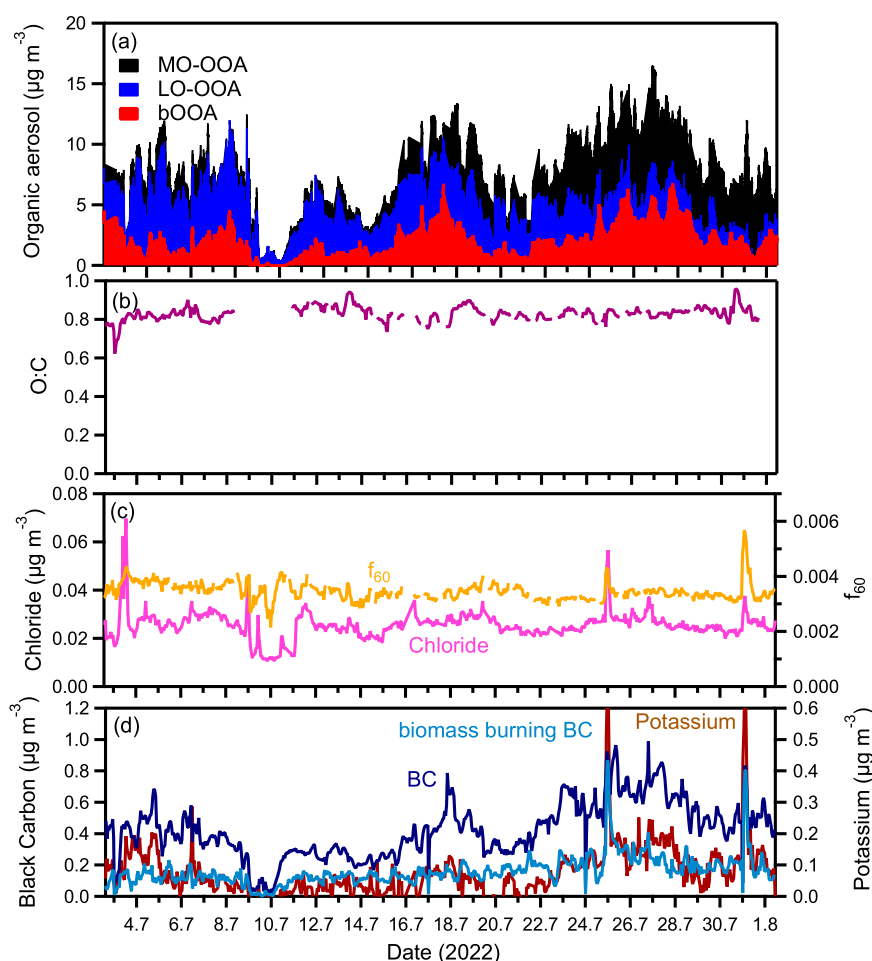


Fig. 1 Aerosol measurements during SPRUCE-22. Time series of: **a** OA components estimated by PMF; **b** organic aerosol oxygen-to-carbon ratio; **c** chloride and f_{60} (biomass burning related fragment fraction); **d** black carbon, biomass burning black carbon and AMS potassium.

RESULTS

Evidence for the influence of fires

A series of biomass-burning tracers and techniques were used to identify the influence of wildfires in this remote site. Potassium is used as an inert non-volatile tracer^{11,12} of biomass-burning OA. On average the $PM_{2.5}$ potassium concentration in Pertouli was $0.2 \mu\text{g m}^{-3}$, and there were specific days that it reached up to $0.4 \mu\text{g m}^{-3}$ (Supplementary Fig. 3). The Aerosol Mass Spectrometer (AMS) measures only a fraction of the potassium¹³ and reported an average concentration of $0.08 \mu\text{g m}^{-3}$.

Dust and sea-salt contributions to the K^+ concentrations were quantified, and biomass burning was found to be the dominant (more than 75%) source of potassium. The average $PM_{2.5}$ biomass burning K^+ was estimated to be $0.15 \mu\text{g m}^{-3}$. The K^+ was associated with the MO-OOA, as the R^2 between the two was equal to 0.61 (daily resolution) (Supplementary Fig. 3). The source apportionment analysis was repeated including potassium in the input matrix. PMF associated 76% of the potassium with the MO-OOA (Supplementary Fig. 4). The remaining 24% was associated with the biogenic factor. This is an indication that biomass-burning secondary OA (bbSOA) is a major part of the MO-OOA at least in this study.

There are no available direct measurements of the levels of levoglucosan during SPRUCE-22. However, the AMS m/z 60 and 73 have been strongly linked to levoglucosan in previous studies¹⁴. During our campaign, the levels of both m/z 60 and m/z 73 were quite low. For example, the f_{60} was just 0.4% on average, more

than order of magnitude lower than the levels expected in an area dominated by fresh biomass burning OA which are up to 6%¹⁵. Values of f_{60} at least 1% are expected to support the presence of fresh biomass-burning OA. This is shown in the f_{44} vs f_{60} triangle plot (Supplementary Fig. 5) in which all our measurement points fall outside the area in which fresh biomass burning OA is usually encountered. Most of the measurements were at the background f_{60} level (0.3%), suggesting strongly that the levoglucosan levels during the campaign were quite low or even negligible. This finding does support our hypothesis that the characteristic chemical fingerprints of biomass-burning OA (including levoglucosan) were rapidly lost during atmospheric aging. Levoglucosan is semivolatile, especially during the summer, a fraction of it is present in the gas phase where it can get rapidly oxidized, leading to evaporation of the remaining levoglucosan from the particulate phase and further oxidation until little levoglucosan can be found in the particles. Part of the products of these reactions are transformed to oxidized OA, which is probably part of the MO-OOA detected in this study.

Black carbon (BC) was on average $0.42 \mu\text{g m}^{-3}$ based on the Aethalometer measurements. Wood burning was estimated¹⁶ to contribute approximately 40% of the BC. The wood burning contribution to BC was even higher at the high-potassium days, exceeding 50% (Supplementary Fig. 6). During those days potassium also had high concentration ($R^2 = 0.58$ between K^+ and biomass burning BC) (Supplementary Fig. 6). The significant contribution of wood burning to black carbon supports the importance of this fine PM source in this area. The water-soluble

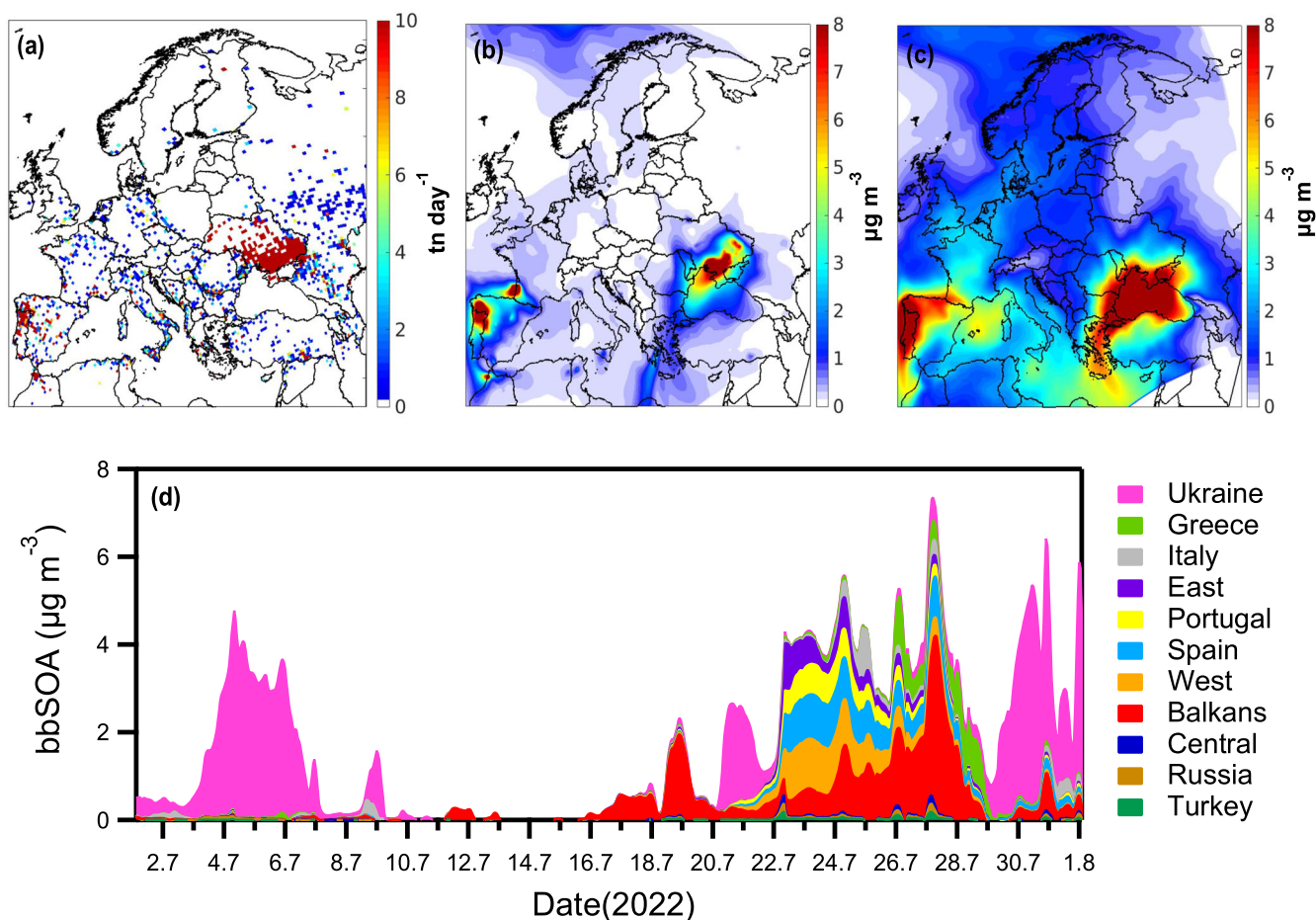


Fig. 2 Wildfire emissions and PMCAM_x-SR results of the bbOA in Europe and Pertouli. **a** PM_{2.5} wildfire emissions for July 2022 (50–500 m), **b** predicted bbPOA in Europe for July 2022, **c** predicted bbSOA in Europe for July 2022, **d** time series of predicted bbSOA in Pertouli and the areas of the corresponding fires shown with different colors.

brown carbon levels measured were insignificant, suggesting considerable processing of the corresponding air masses and photo-bleaching of the water-soluble brown carbon¹⁷.

The contribution of biomass burning to OA in the site was also estimated using the PMCAM_x-SR chemical transport model¹⁸ (Fig. 2). It was predicted that secondary biomass burning OA was responsible for around 40% and primary biomass burning for 4% of the total OA (Supplementary Fig. 7). This estimated biomass burning contribution is high considering that it is for a site far away from wildfires.

Fire case studies

Nearby fires. The measured K⁺ and BC levels both peaked on July 25 and July 31 (Fig. 3). Higher levels of chloride were also measured. The *f*₆₀, which is a biomass-burning tracer, also increased in these days (Supplementary Fig. 8). Analysis of the air mass trajectories (Supplementary Fig. 9) suggested that during the first period, the site was influenced by a major fire in Dadia (northeast Greece, approximately 400 km from the site). During the second period, another fire in Albania (approximately 150 km from the site) was affecting the site. We estimated using HYSPLIT¹⁹ that the fire emissions travelled 2 days before reaching the site during the first fire event and 1 day during the second fire event.

The MO-OOA, which was the most aged factor among the three, increased during these two periods reaching approximately 10 µg m⁻³ (Fig. 3). During the first period the MO-OOA concentration increased by 4 µg m⁻³, the bOOA by 0.4 µg m⁻³ and the LO-OOA remained constant. During the second period the MO-OOA

concentration increased by 3.1 µg m⁻³, the LO-OOA by 0.5 µg m⁻³ and the bOOA concentration remained constant and at low levels. In both cases the MO-OOA was responsible for most of the OA increase in these periods during which the site was clearly affected by wildfire emissions.

Using the ME-2 algorithm, the additional OA during the two periods was attributed to both bbPOA and MO-OOA. The MO-OOA concentration was approximately 10 times more than that of the bbPOA during the first and 6 times during the second period. This strongly suggests that more than 80% of the biomass burning OA had been transformed to MO-OOA during the 1–2 days of transport of the fire emissions to the measurement site.

The MO-OOA correlated well (*R*² = 0.74 for hourly values) with the AMS potassium during these events. This is additional evidence that biomass burning emissions had been transformed to MO-OOA during these periods in which the fire impact on the site was quite clear. A good agreement between MO-OOA and K⁺ has also been reported before²⁰ in the southwestern United States during winter and was attributed to aged biomass burning emissions.

Both the *m/z* 60 and nitrate followed the same trend with MO-OOA during the fire case study periods. A stronger link between *m/z* 60 and MO-OOA is expected when some fresh biomass-burning OA remains in the aerosol. This link is expected to weaken and eventually disappear as the OA ages. Our results support this view. The *R*² between the MO-OOA and the *m/z* 60 for the whole month was 0.33. The correlation was better for the two brief fire periods, as the *R*² increased to 0.9 (Supplementary Fig. 10). Nitrate

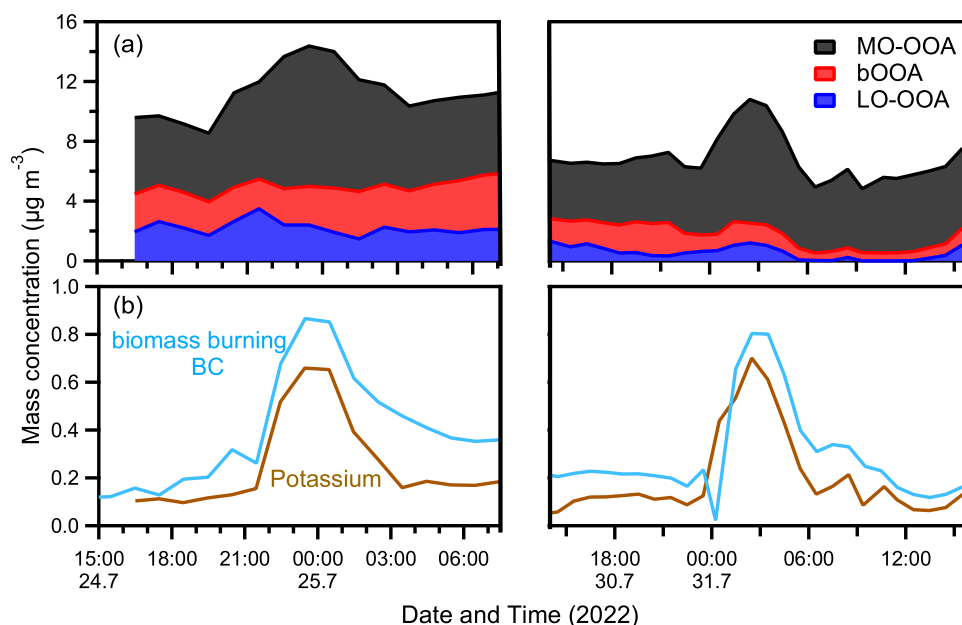


Fig. 3 Timeseries of aerosol components. Timeseries of aerosol components for the two case studies (24/7–25/7 Dadia fire) and (30/7–31/7 Albania fire) of the **a** organic factors and **b** potassium and biomass burning black carbon.

(which was mostly organic) had a similar behavior. MO-OOA had an R^2 equal to 0.17 with nitrate (1-h resolution) for the study and 0.84 for the two fire periods (24–25/7 and 30–31/7) (Supplementary Fig. 11). The MO-OOA factor had little average diurnal variation which is a typical behavior for a highly oxidized OA component that has been transported over relatively long distances (Supplementary Fig. 12).

The difference of these two fires compared to the rest is that they occurred relatively close to the sampling site (1–2 days of transport time and 150–400 km away) so their effect could be captured by the auxiliary measurements.

Fires in Portugal. The PMCAMx-SR results showed that the bbSOA in Pertouli originated from wildfires which occurred in various areas of Europe (Fig. 2). Major fires in Portugal started on July 7 and lasted until the end of the month (Supplementary Fig. 13). Their emissions traveled through many European countries such as the United Kingdom, France, Germany, Norway, etc. and reached this remote site in Greece two weeks later (July 21). The Iberian Peninsula fires, which originated thousands of kilometers away from Greece, were responsible for a significant fraction of the bbSOA in the site for the period July 21 to July 31 according to PMCAMx-SR. Except from the fires in Spain and Portugal, the bbSOA in Pertouli was also affected by fires in Ukraine, Italy, and the Balkans according to PMCAMx-SR.

Biomass burning organic aerosol levels

The quantification of the bbOA concentration is challenging due to its aging. For that reason, we rely on the combination of different indirect methods. First, the measured potassium concentrations can be used for the calculation. The fresh bbOA:K⁺ concentration ratio in the literature varies from 5 to 100 with an average value of 20^{21–24}. The ratio could be higher if bbOA levels increase during aging. Using these three ratios (5 and 100 for the extremes and 20 for the expected value) the bbOA in the site should be on average 3 µg m⁻³ (range 0.75–15 µg m⁻³) or 40% of the total OA (range 10–100%). For the upper limit, the bbOA estimated exceeds the total OA measured, so we use 100% of the OA instead.

Even though potassium has been used in several studies as a biomass-burning tracer²⁵ there are also some studies which indicate that use of K⁺ can lead to over-prediction of bbOA especially during summer²⁶. However, these studies have focused on primary bbOA and not on the secondary, which was the dominant form of bbOA in our study. The problem lies in neglecting the transformation of fresh biomass-burning OA to aged highly oxidized OA that is then not associated with biomass-burning aerosol. Therefore, even if these studies using K⁺ probably provide reasonable estimates of the contribution of total (fresh and oxidized) bbOA, provided that there are no other significant sources of K⁺ in the analyzed samples, they conclude that bbOA is overestimated. The discrepancy is due to the fact that the potentially significant levels of processed bbOA are neglected. So indeed, use of K⁺ leads to an overestimation of the fresh bbOA, but such estimates are probably much better indicators of the total bbOA, especially if one can account for the aging processes. The contribution of other sources (dust, sea-salt) to the potassium concentration in our case was quite low.

PMCAMx-SR predicted that 55% of the OA was due to fires in the modeling domain and another 21% due to transport from outside the domain. The measured MO-OOA was in reasonable agreement with the sum of bbSOA and long-range transport (LRT) OA (Supplementary Fig. 14). This supports our hypothesis that a significant fraction of the biomass burning OA is part of the MO-OOA measured by the AMS. However, the model tended to underestimate OA, so its predictions could be viewed as a lower bound of the true biomass burning contribution. Part of this underestimation may be the estimation of wildfire emissions. Fire emission estimates are quite uncertain and the IS4FIRES values used in this work differ compared to other fire emission inventories by at least a factor of 2. Depending on the area and the period modeled the values in the various fire inventories can be higher than those in IS4FIRES used here²⁷.

The PM_{2.5} mass concentration was practically the same (within a few µg m⁻³ at daily resolution) as in Pertouli in different areas in Greece during July 2022 including Athens, Thessaloniki, Patras (Supplementary Fig. 15). This is consistent with the regional influence of the secondary bbOA from fires mostly outside Greece.

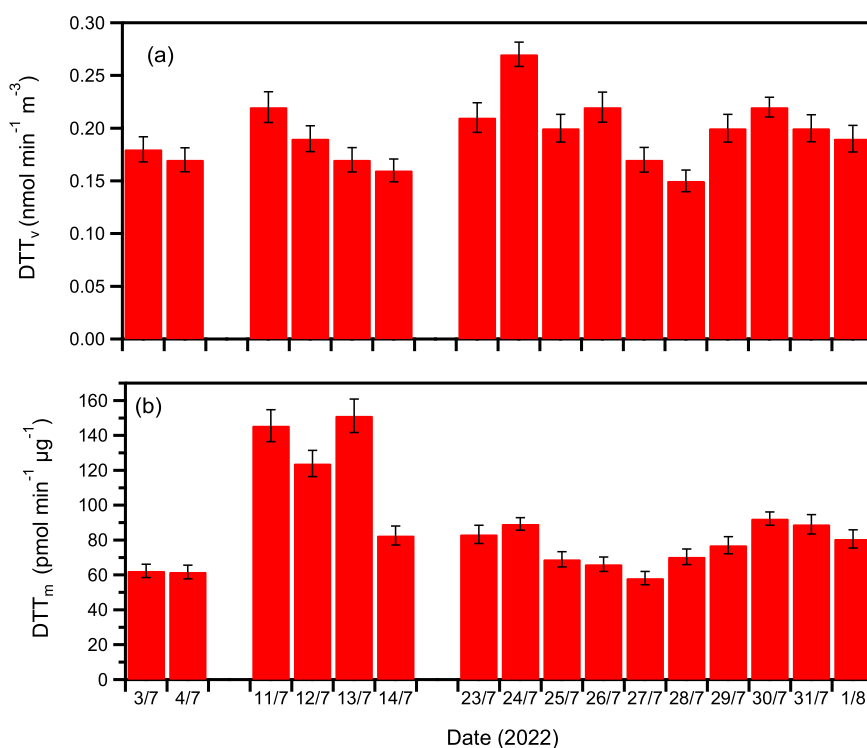


Fig. 4 Daily average oxidative potential of the water-soluble particulate matter during the study. **a** DTT (per unit air volume) and **b** DTT (per unit mass). The error bars represent the standard deviation.

PMCAMx predicted an average bbSOA concentration of $2 \mu\text{g m}^{-3}$ over Europe (Fig. 2). This appears to be a conservative estimate given that the model at least in Pertouli predicts lower OA and bbSOA levels compared to the estimates based on the measurements.

Oxidative potential of particulate matter

Oxidative potential (OP) has been linked to the PM-bound and/or induced reactive oxygen species and their ability to cause oxidative stress and damage to biological systems^{28,29}. It is widely used as a metric of potential aerosol toxicity^{30,31}. The OP of the water-soluble PM_{2.5} fraction was measured using the acellular dithiothreol (DTT) assay^{32,33}. This water-soluble fraction is expected to include practically all the OA given its highly oxidized state³⁴. The DTT assay has been extensively used in previous field studies both in Europe (including Greece) and the US and therefore there is a good set of other measurements for comparison.

The annual average DTT_m (OP per unit mass) of fine PM in Europe ranges between $6\text{--}30 \text{ pmol min}^{-1} \mu\text{g}^{-1}$ for urban background sites and between 9 and $22 \text{ pmol min}^{-1} \mu\text{g}^{-1}$ for rural areas³⁵. In Athens, Greece³⁶ the annual average DTT_m is $28 \pm 14 \text{ pmol min}^{-1} \mu\text{g}^{-1}$. Lower OP values ($10 \text{ pmol min}^{-1} \mu\text{g}^{-1}$) have been reported for a suburban central Mediterranean site (Salento's peninsula, South Italy) during summer³⁷. Atmospheric processing affects the OP of ambient OA³⁸ with DTT_m values of oxidized OA^{20,35} ranging between $20\text{--}60 \text{ pmol min}^{-1} \mu\text{g}^{-1}$. The lower values have been reported in south Mediterranean background areas during summer. For example, the DTT_m of aged OA (more than 1 d of transport time) during summer in Greece, was measured at $22 \text{ pmol min}^{-1} \mu\text{g}^{-1}$; two times higher than that of the fresh OA ($10 \text{ pmol min}^{-1} \mu\text{g}^{-1}$) with less than 5 h of transport time³⁸. The average DTT_m in this study was $84 \pm 27 \text{ pmol min}^{-1} \mu\text{g}^{-1}$ (Fig. 4), which is higher than the average values reported in the literature for oxidized OA in Mediterranean sites during summer.

The average DTT_v (per unit volume of air) during SPRUCE-22 was $0.2 \pm 0.03 \text{ nmol min}^{-1} \text{ m}^{-3}$ (Fig. 4). Similar levels ($0.2 \pm 0.05 \text{ nmol min}^{-1} \text{ m}^{-3}$ average annual DTT_v) have been observed in ten European sites, including regional background, urban background, and urban traffic locations³⁹ as well as in a central Mediterranean site during summer³⁷, where DTT_v was equal to $0.19 \pm 0.02 \text{ nmol min}^{-1} \text{ m}^{-3}$. Multiple linear regression was performed to the SPRUCE-22 DTT_v measurements, to estimate which PMF factor affects more the results. Among the different types of OA in the site, the MO-OOA was the one which influenced the most the measured DTT_v reactivity, while practically zero contribution was estimated for biogenic OOA. These results suggest that the oxidized OA in the site had OP that is at least equal and probably higher than the average OA in Europe.

DISCUSSION

Many epidemiological studies consider fine PM_{2.5} to be the highest environmental risk to human health, leading to cardiovascular and respiratory diseases. Both long-term and short-term exposure to even low concentrations of PM_{2.5} leads to an increase in mortality^{40–42}. PM_{2.5} explicitly from fresh biomass burning emissions has also been linked to mortality excess risk^{43–45}.

A linear relationship between the exposure to ambient PM and mortality has been assumed for the relatively modest fine PM levels involved. The average slope used is based on a series of epidemiological studies that assume a similar linear relationship. Another assumption of our estimation is that the corresponding aged biomass burning OA is at least as dangerous as the average fine PM in Europe. This simplification allows us to use the results of past detailed epidemiological analyses in Europe.

The average bbSOA due to wildfires over Europe during the study period is estimated to be around $2\text{--}3 \mu\text{g m}^{-3}$ based on the model and the measurements. As a result, hundreds of millions of people were exposed to the corresponding particles that appear to be quite toxic. These particles remain in the atmosphere for

several days and can travel thousands of kilometers away from the corresponding fire. Assuming a linear relationship between the exposure to ambient PM and mortality, and the average number of deaths in Europe due to ambient air pollution (300,000), we estimate that exposure to these levels can lead to 3600–5400 premature deaths per month. Assuming similar levels for the rest of the summer, these correspond to 10,800–16,200 premature deaths during each summer.

Even if these deaths are included in the approximately 300,000 deaths per year in Europe as the result of exposure to ambient fine particulate matter⁴⁶, they have not been associated with summertime biomass burning. The results of this study indicate that 15–22 out of 100 deaths from ambient PM exposure in Europe during summer are associated with biomass burning from wildfires. A more comprehensive estimate of these health effects is possible with the use of multiple summer periods, fire emission inventories, and bbOA aging models.

METHODS

M1. Source apportionment analysis

For the source apportionment of OA positive matrix factorization (PMF) analysis was performed with temporal resolution of 3 minutes. The “weak” (signal to noise ratio 0.2–2) and “bad” variables (signal-to-noise ratio below 0.2) were treated, while the CO₂-related variables were also down-weighted⁴⁷. Solutions from 1 up to 5 factors were explored for F_{peak} values in the –1 to 1 range exploring the effects of the rotation of the solution. The three-factor solution was chosen. Both the 4- and the 5-factor solutions included non-meaningful factors, so they were discarded. Diagnostic plots related to the 2-factor solution and the 3-factor solution are shown in Supplementary Fig.16. The OA factor AMS spectra derived from the chosen solution were compared with reference spectra in the literature. The biogenic OOA was characterized by m/z 's 53 and 82, which are biogenic tracers⁴⁸. The MO-OOA and LO-OOA factors were compared to the ones from FAME-2008 which also correspond to a background site in Greece and the θ angle was below 15° in each case⁴⁹.

The diurnal profiles of the three factors did not show significant variation which is the typical behavior of highly aged aerosol. Only LO-OOA had a minor peak around 14:00 (local time) possibly due to increased photo-chemical activity.

As a sensitivity analysis, the Multilinear Engine (ME-2) was used to quantify the concentration of bbPOA. A fresh bbOA spectrum was used for constraining the solution. The a -value varied from 0 up to 1. The solution presented here is for $a = 0$, given that we are trying to quantify the fresh bbPOA. For $a = 0.5$, the resulting bbOA spectrum corresponded to aged biomass burning OA. The bbOA contribution to the total OA in this case was 6%.

The MO-OOA seems to include a significant fraction of the bbSOA as it had the same trend with the potassium ($R^2 > 0.85$) and other biomass burning tracers in the examined periods in which the site was affected by the Dadia and the Albania fires. The concentration of MO-OOA was approximately 5 times more than that of the bbPOA in these fire events indicating that at least 80% of the bbOA was of secondary origin, even in these cases in which the fire emissions had spent only 1–2 days in the atmosphere. For longer residence times the primary bbOA contribution was below detection levels.

M2. Fire-case studies

The average OA AMS spectrum during the Dadia and Albanian fire periods was compared those during the rest of the study and no significant differences were observed ($\theta < 12^\circ$). The f_{60} during these fires was on average 0.5% which is in the background range. On average it was even lower at 0.4%. This shows that the bbOA

emitted by the wildfires was highly processed before it reached the site. Consequently, the bbOA AMS signature was lost.

The C₁₀H₁₃O₃⁺, which has been identified as a biomass-burning tracer¹⁰ during aging chamber experiments, also increased during the fire events. However, its concentration was still low and resulted in minor differences in the OA spectrum.

The first fire in Dadia, Greece started on July 21 and stayed active until July 27. Air trajectories using the Hybrid Single-Particle Lagrangian Integrated Trajectory model (HYSPPLIT) showed that the air masses passed near the fire in the afternoon of July 22 and reached the Pertouli site on July 24, approximately two days later (Supplementary Fig. 9). During the same period air masses that had originated in Portugal were also moving south to the Balkans based on PMCAMx-SR. The emissions of the fire in Dadia were therefore added on top of the highly processed bbOA due to the Iberian fires. On July 25 at 01:00 the potassium and wood-burning BC concentrations started to drop even though the fire was still active. This was because the air changed direction and the air masses arriving in Pertouli did not pass close to the fire area.

The second fire occurred in Albania on July 30 and 31. Air masses passed over the area of the fire and reached Pertouli after one day. The fire occurred relatively close to the site (150 km); however, wind velocities were low during that period and the air masses moved slowly to the site. Our results indicate that even in the 1 d required for the transport of the plume to the site practically all (>80%) of the fresh bbOA was aged. The smaller distance compared to the other fires and the weak dilution may be responsible for the K⁺ and biomass burning BC peaks in the observations.

M3. Potassium sources

In this work, the potassium has been used as a biomass burning tracer. However, potassium can have other sources in the atmosphere, such as sea salt and dust. In this work the PM_{2.5} K⁺ was measured, while dust and sea-salt K⁺ is mostly found in the coarse mode, so low contributions of these two sources are expected. Nevertheless, the biomass burning fraction of K⁺ was quantified for more accurate results.

In a first step the non-sea salt potassium was calculated using two methods. In the first method^{50,51} the Na⁺ concentration was used assuming that $K^+_{\text{sea-salt}} = 0.0355 \text{ Na}^+$. In the second the Mg⁺² ($K^+_{\text{sea-salt}} = 0.3082 \text{ Mg}^{+2}$) was used⁵². Both methods showed that the sea-salt K⁺ concentration was low (0.01 $\mu\text{g m}^{-3}$ on average) and practically all the potassium was of non-sea salt origin. This behavior applies also for the fire cases and not only for the average period.

The contribution of dust to the potassium concentration was also quantified. In that case the Ca⁺² concentration was used. The dust K⁺ was calculated as $K^+_{\text{dust}} = 0.2 \text{ Ca}^{+2}$, where the slope (0.2) stands for the average K⁺: Ca⁺² ratio in dust^{53–58}. The K⁺_{dust} was equal to 0.04 $\mu\text{g m}^{-3}$ in this study.

Since the sea-salt and the dust K⁺ concentrations were quantified, the biomass burning potassium was calculated according to:

$$K^+_{\text{bb}} = K^+ - K^+_{\text{sea-salt}} - K^+_{\text{dust}}$$

The average PM_{2.5} biomass burning K⁺ concentration was 0.15 $\mu\text{g m}^{-3}$.

M4. Estimation of total bbOA in Pertouli

The potassium concentration was used as the basis for the estimation of the bbOA levels in Pertouli. The bbOA:K⁺ ratio has been used in previous studies to estimate biomass burning aerosol concentrations and emissions with reported values in the 5–100 range. The value of the ratio depends on both the burning conditions and aging⁵⁹.

For the bbOA calculation in Pertouli, we assume an average bbOA:K⁺ ratio equal to 20²². Based on the average PM_{2.5} biomass burning K⁺ concentration for July 2022 (0.15 µg m⁻³) we calculated that the average bbOA concentration was equal to 3 µg m⁻³. The bbOA concentration can range between 0.75 and 15 µg m⁻³ if we use the lower and upper limits of the bbOA:K ratio found in literature (5 and 100). If we use the AMS K⁺, the bbOA concentration is estimated to be 1.5 µg m⁻³, which is an underestimation of the total bbOA given that the AMS measures only a fraction of the K⁺. The estimated bbOA concentration in Pertouli by PMCAMx-SR was 2 µg m⁻³, which is probably also a low estimate given the underprediction of the OA by the model. We use as our best estimate the average of the measurement-based estimate and the model predictions to conclude that the average total bbOA concentration in Pertouli during the study was 2–3 µg m⁻³ based on the two estimates.

M5. PMCAMx-SR

The source resolved version of the Particulate Matter Comprehensive Air quality Model with extensions (PMCAMx-SR) is an extension of PMCAMx which can simulate explicitly the OA from biomass burning¹⁸. In the current study we applied PMCAMx-SR over Europe covering a region of 5400 × 5832 km² described by a polar stereographic map projection using a 36 × 36 km horizontal resolution and 14 vertical layers which extend almost up to 6 km. All meteorological fields used as inputs for PMCAMx-SR were generated by the Weather Research and Forecast Model v4.1.5 (WRF)⁶⁰. The simulations were performed from June 28 to July 31, 2022, excluding the first three days to minimize the effect of the initial conditions.

The wildfire emissions used by PMCAMx-SR, were based on the IS4FIRES emissions³ provided by the Finnish Meteorological Institute. PMCAMx-SR is using the Volatility Basis Set (VBS) approach to describe the OA⁶¹. A volatility distribution specific to wildfire emissions is used⁶². PMCAMx-SR also needs other categories of emissions like biogenic, marine, and anthropogenic emissions. Biogenic emissions⁶³ were produced by the Model of Emissions of Gases and Aerosols from Nature v3 (MEGAN), marine emissions are based on the algorithms of O'Dowd et al.⁶⁴ and Monahan et al.⁶⁵ and anthropogenic emissions are based on the TNO emission inventory⁴.

M6. Oxidative potential

Sixteen daily PM_{2.5} samples were collected to quantify the water-soluble oxidative potential (WS-OP). Pre-backed quartz filters (Whatman; QMA, 101.6 mm) were used together with a medium-volume air sampler (Tisch Environmental, model TE-1000) operating at 170 L min⁻¹, that was coupled with a set of two cyclones. All samples were stored at -20 °C until analysis. Measurements of WS-OP of the samples were performed using a semi-automated system³³ that is programmed to operate running an optimized version of the acellular dithiothreol (DTT) assay³². The WS-OP is calculated by subtracting the DTT consumption rate of a blank sample, that accounts for any non-specific reactions or interference, from the DTT consumption rate of the samples. The net DTT consumption rates of the samples were expressed either in nmol min⁻¹ m⁻³ (volume normalized DTT activity – DTT_v), considering the sampling air flow of the analyzed PM samples, or in pmol min⁻¹ µg⁻¹ (OC mass normalized DTT activity – DTT_m) representing the source-related intrinsic property of particles. For precision control purposes of the semi-automated system, a phenanthroquinone (PQN) solution was used as an external standard, for each analyzed sequence of samples.

In order to identify which sources contributed most to the OP of the site, a multiple linear regression of the DTT_v values (16 samples) with the PMF factors and the metals identified was performed. The metals analysis was performed by X-ray

fluorescence (XRF). The DTT_v was expressed as follows:

$$DTT_v = a(\text{bOOA}) + b(\text{LO} - \text{OOA}) + c(\text{MO} - \text{OOA}) + \sum d(\text{elements}) + k$$

The results showed limited correlation of the OP measurements with the bOOA and the LO-OOA as the coefficients of the regression were almost zero. The highest coefficient among the three factors was observed for the most aged factor (MO-OOA). Among the elements, K⁺ and Cl⁻ (both related to biomass burning) affected the OP measurements significantly. The R² between the observed and the predicted OP was 0.6.

M7. Estimation of the bbOA health effects

There are many epidemiological studies which address the excess mortality in Europe due to PM_{2.5}. The annual number of deaths in Europe due to outdoor exposure to PM_{2.5} has been estimated to be approximately 300,000, while the annual mean PM_{2.5} concentration in Europe⁶⁶ is 14 µg m⁻³. This corresponds (using the linear response assumed in the corresponding epidemiological study) to 21,400 deaths per µg m⁻³ of annual exposure or 1800 deaths per µg m⁻³ for monthly exposure.

The average total bbOA concentration over Europe predicted by PMCAMx-SR was 2 µg m⁻³ (Fig. 2). With this assumption we estimate approximately 10,800 deaths per summer in Europe due to ambient exposure to secondary biomass burning aerosol. This corresponds to approximately 15% of the total deaths during summer due to exposure to outdoor particulate matter. This is probably a conservative estimate given the tendency of the model to underpredict the bbOA in Pertouli by 50%. Correcting for this 50% underprediction we can estimate an upper limit of the bbOA at 3 µg m⁻³ which corresponds to 16,200 deaths during summer. The results of this study show that 15–22 out of 100 deaths in Europe due to particulate matter during summer are due to exposure to bbOA and mainly its secondary component.

DATA AVAILABILITY

The dataset is publicly accessible at <https://doi.org/10.5281/zenodo.10396713>. The data of the current study are restricted. They can be available from the corresponding author (Spyros N. Pandis) on reasonable request.

CODE AVAILABILITY

The PMCAMx-SR source code is available at: zenodo.org/record/4071362.

Received: 25 September 2023; Accepted: 5 December 2023;
Published online: 21 December 2023

REFERENCES

- Majdi, M. et al. Impact of wildfires on particulate matter in the Euro-Mediterranean in 2007: sensitivity to some parameterizations of emissions in air quality models. *Atmos. Chem. Phys.* **19**, 785–812 (2019).
- Sofiev, M. et al. An operational system for the assimilation of the satellite information on wild-land fires for the needs of air quality modelling and forecasting. *Atmos. Chem. Phys.* **9**, 6833–6847 (2009).
- Chen, G. et al. European aerosol phenomenology – 8: Harmonised source apportionment of organic aerosol using 22 Year-long ACSM/AMS datasets. *Environ. Int.* **166**, 107325 (2022).
- Kuener, J. J. P., Visschedijk, A. J. H. & Jozwicka, M. & Denier Van Der Gon, H. A. C. TNO-MACC_II emission inventory; a multi-year (2003–2009) consistent high-resolution European emission inventory for air quality modelling. *Atmos. Chem. Phys.* **14**, 10963–10976 (2014).
- Paatero, P. & Tapper, U. Positive matrix factorization: A non-negative factor model with optimal utilization of error estimates of data values. *Environmetrics* **5**, 111–126 (1994).
- Jayne, J. T. et al. Development of an Aerosol Mass Spectrometer for size and composition analysis of submicron particles. *Aerosol Sci. Tech.* **33**, 49–70 (2010).

7. Canonaco, F., Crippa, M., Slowik, J. G., Baltensperger, U. & Prévôt, A. S. H. SoFi, an IGOR-based interface for the efficient use of the generalized multilinear engine (ME-2) for the source apportionment: ME-2 application to aerosol mass spectrometer data. *Atmos. Meas. Tech.* **6**, 3649–3661 (2013).
8. Vasilakopoulou, C. N. et al. Development and evaluation of an improved offline aerosol mass spectrometry technique. *Atmos. Meas. Tech.* **16**, 2837–2850 (2023).
9. Robinson, A. L. et al. Rethinking organic aerosols: Semivolatile emissions and photochemical aging. *Science* **315**, 1259–1262 (2007).
10. Yazdani, A. et al. Chemical evolution of primary and secondary biomass burning aerosol during daytime and nighttime. *Atmos. Chem. Phys.* **23**, 7461–7477 (2023).
11. Halstead, H. D. Saturated vapour pressure of potassium sulphate. *Trans. Faraday Soc.* **66**, 1966–1973 (1970).
12. Bradley, R. S. & Volans, P. Rates of evaporation IV. The vapour pressure and rate of evaporation of potassium chloride. *Proc. R. Soc. Lond. Ser. A. Math. Phys. Sci.* **217**, 508–523 (1953).
13. Takegawa, N. et al. Performance of an Aerodyne Aerosol Mass Spectrometer (AMS) during intensive campaigns in China in the summer of 2006. *Aerosol Sci. Technol.* **43**, 189–204 (2009).
14. Saarnio, K. et al. Online determination of levoglucosan in ambient aerosol with particle-into-liquid sampler-high-performance anion-exchange chromatography-mass spectrometry (PILS-HPAEC-MS). *Atmos. Meas. Tech.* **6**, 2839–2849 (2013).
15. Milic, A. et al. Biomass burning and biogenic aerosols in northern Australia during the SAFIRED campaign. *Atmos. Chem. Phys.* **17**, 3945–3961 (2017).
16. Sandradewi, J. et al. Using aerosol light absorption measurements for the quantitative determination of wood burning and traffic emission contribution to particulate matter. *Environ. Sci. Technol.* **42**, 3316–3323 (2008).
17. Forrister, H. et al. Evolution of brown carbon in wildfires plumes. *Geophys. Res. Lett.* **42**, 4623–4630 (2015).
18. Theodoritsi, G. N. & Pandis, S. N. Simulation of the chemical evolution of biomass burning organic aerosol. *Atmos. Chem. Phys.* **19**, 5403–5415 (2019).
19. Draxler, R. R. & Hess, G. D. An overview of the HYSPLIT_4 modelling system for trajectories, dispersion and deposition. *Aust. Meteorol. Mag.* **47**, 295–308 (1998).
20. Verma, V. et al. Organic aerosols associated with the generation of reactive oxygen species (ROS) by water-soluble PM2.5. *Environ. Sci. Technol.* **49**, 4646–4656 (2015).
21. Lee, A. K. Y. et al. Single-particle characterization of biomass burning organic aerosol (BBOA): Evidence for non-uniform mixing of high molecular weight organics and potassium. *Atmos. Chem. Phys.* **16**, 5561–5572 (2016).
22. Seinfeld, J. H. & Pandis, S. N. *Atmospheric Chemistry and Physics: From Air Pollution to Climate Change* (John Wiley & Sons), (2016).
23. Park, S. S., Jung, S. A., Gong, B. J., Cho, S. Y. & Lee, S. J. Characteristics of PM2.5 haze episodes revealed by highly time-resolved measurements at an air pollution monitoring supersite in Korea. *Aerosol Air Qual. Res.* **13**, 957–976 (2013).
24. Chow, J. Measurement methods to determine compliance with ambient air quality standards for suspended particles. *J. Air Waste Manag. Assoc.* **45**, 320–382 (2012).
25. Jing, B. et al. Hygroscopic properties of potassium chloride and its internal mixtures with organic compounds relevant to biomass burning aerosol particles. *Sci. Rep.* **7**, 43572 (2017).
26. Pachon, J. E., Weber, R. J., Zhang, X., Mulholland, J. A. & Russell, A. G. Revising the use of potassium (K) in the source apportionment of PM2.5. *Atmos. Pollut. Res.* **4**, 14–21 (2013).
27. Jin, Y. et al. Measurement report: Assessing the impacts of emission uncertainty on aerosol optical properties and radiative forcing from biomass burning in peninsular southeast Asia. *EGUsphere*, 1–43, <https://doi.org/10.5194/egusphere-2023-1650> (2023).
28. Guascito, M. R. et al. Characterisation of the correlations between oxidative potential and in vitro biological effects of PM10 at three sites in the central Mediterranean. *J. Hazard. Mater.* **448**, 130872 (2023).
29. Jiang, H., Ahmed, C. S., Canchola, A., Chen, J. Y. & Lin, Y. H. Use of dithiothreitol assay to evaluate the oxidative potential of atmospheric aerosols. *Atmosphere* **10**, 571 (2019).
30. Yadav, S. & Phuleria, H. C. Oxidative potential of particulate matter: A prospective measure to assess PM toxicity. *Energy, Environment, and Sustainability*, 333–356 (2020).
31. Zhang, Z. H. et al. Are reactive oxygen species (ROS) a suitable metric to predict toxicity of carbonaceous aerosol particles? *Atmos. Chem. Phys.* **22**, 1793–1809 (2022).
32. Cho, A. K. et al. Redox activity of airborne particulate matter at different sites in the Los Angeles Basin. *Environ. Res.* **99**, 40–47 (2005).
33. Fang, T. et al. A semi-automated system for quantifying the oxidative potential of ambient particles in aqueous extracts using the dithiothreitol (DTT) assay: Results from the Southeastern Center for Air Pollution and Epidemiology (SCAPE). *Atmos. Meas. Tech.* **8**, 471–482 (2015).
34. Liangou, A. et al. A method for the measurement of the water solubility distribution of atmospheric organic aerosols. *Environ. Sci. Technol.* **56**, 3952–3959 (2022).
35. Shafer, M. M., Hemming, J. D. C., Antkiewicz, D. S. & Schauer, J. J. Oxidative potential of size-fractionated atmospheric aerosol in urban and rural sites across Europe. *Faraday Discuss.* **189**, 381–405 (2016).
36. Paraskevopoulou, D. et al. Yearlong variability of oxidative potential of particulate matter in an urban Mediterranean environment. *Atmos. Environ.* **206**, 183–196 (2019).
37. Perrone, M. R. et al. PM2.5 and PM10 oxidative potential at a Central Mediterranean Site: Contrasts between dithiothreitol- and ascorbic acid-measured values in relation with particle size and chemical composition. *Atmos. Environ.* **210**, 143–155 (2019).
38. Wong, J. P. S. et al. Effects of atmospheric processing on the oxidative potential of biomass burning organic aerosols. *Environ. Sci. Technol.* **53**, 6747–6756 (2019).
39. Jedynska, A. et al. Spatial variations and development of land use regression models of oxidative potential in ten European study areas. *Atmos. Environ.* **150**, 24–32 (2017).
40. Stafoggia, M. et al. Long-term exposure to low ambient air pollution concentrations and mortality among 28 million people: results from seven large European cohorts within the ELAPSE project. *Lancet Planet. Heal.* **6**, e9–e18 (2022).
41. Southerland, V. A. et al. Global urban temporal trends in fine particulate matter (PM2.5) and attributable health burdens: estimates from global datasets. *Lancet Planet. Heal.* **6**, e139–e146 (2022).
42. Liu, C. et al. Ambient particulate air pollution and daily mortality in 652 cities. *N. Engl. J. Med.* **381**, 705–715 (2019).
43. Karanasiou, A. et al. Short-term health effects from outdoor exposure to biomass burning emissions: A review. *Sci. Total Environ.* **781**, 146739 (2021).
44. Chen, G. et al. Mortality risk attributable to wildfire related PM2.5 pollution: a global time series study in 749 locations. *Lancet Planet. Heal.* **5**, e579–e587 (2021).
45. Chen, J. et al. A review of biomass burning: Emissions and impacts on air quality, health and climate in China. *Sci. Total Environ.* **579**, 1000–1034 (2017).
46. Khomenko, S. et al. Premature mortality due to air pollution in European cities: a health impact assessment. *Lancet Planet. Heal.* **5**, e121–e134 (2021).
47. Ulbrich, I. M., Canagaratna, M. R., Zhang, Q., Worsnop, D. R. & Jimenez, J. L. Interpretation of organic components from Positive Matrix Factorization of aerosol mass spectrometric data. *Atmos. Chem. Phys.* **9**, 2891–2918 (2009).
48. Kostenidou, E. et al. Sources and chemical characterization of organic aerosol during the summer in the eastern Mediterranean. *Atmos. Chem. Phys.* **15**, 11355–11371 (2015).
49. Hildebrandt, L. et al. Aged organic aerosol in the Eastern Mediterranean: the Finokalia Aerosol Measurement Experiment-2008. *Atmos. Chem. Phys.* **10**, 4167–4186 (2010).
50. Lai, S. C., Zou, S. C., Cao, J. J., Lee, S. C. & Ho, K. F. Characterizing ionic species in PM2.5 and PM10 in four Pearl River Delta cities, South China. *Environ. Sci.* **19**, 939–947 (2007).
51. Cao, F., Zhang, S. C., Kawamura, K. & Zhang, Y. L. Inorganic markers, carbonaceous components and stable carbon isotope from biomass burning aerosols in Northeast China. *Sci. Total Environ.* **572**, 1244–1251 (2016).
52. Fourtziou, L. et al. Multi-tracer approach to characterize domestic wood burning in Athens (Greece) during wintertime. *Atmos. Environ.* **148**, 89–101 (2017).
53. Falkovich, A. H. & Schkolnik, G. Adsorption of organic compounds pertinent to urban environments onto mineral dust particles. *J. Geophys. Res.* **109**, D02208 (2004).
54. Wang, Y., Zhuang, G., Sun, Y. & An, Z. The variation of characteristics and formation mechanisms of aerosols in dust, haze and clear days in Beijing. *Atmos. Environ.* **40**, 6579–6591 (2006).
55. Ho, K. F., Lee, S. C., Chow, J. C. & Watson, J. G. Characterization of PM10 and PM2.5 source profiles for fugitive dust in Hong Kong. *Atmos. Environ.* **37**, 1023–1032 (2003).
56. Zhang, R., Shen, Z., Cheng, T., Zhang, M. & Liu, Y. The elemental composition of atmospheric particles at Beijing during Asian dust events in Spring 2004. *Aerosol Air Qual. Res.* **10**, 67–75 (2010).
57. Shen, Z. et al. Ionic composition of TSP and PM2.5 during dust storms and air pollution episodes at Xi'an, China. *Atmos. Environ.* **43**, 2911–2918 (2009).
58. Kchik, H., Perrino, C. & Cherif, S. Investigation of desert dust contribution to source apportionment of PM10 and PM2.5 from a southern Mediterranean coast. *Aerosol Air Qual. Res.* **15**, 454–464 (2015).
59. Zotter, P. et al. Radiocarbon analysis of elemental and organic carbon in Switzerland during winter-smog episodes from 2008–2012. Part 1: Source apportionment and spatial variability. *Atmos. Chem. Phys.* **14**, 13551–13570 (2014).
60. Skamarock, W. C. et al. A description of the Advanced Research WRF Model Version 4.1; No. NCAR/TN-556+STR; National Center for Atmospheric Research: Boulder, CO, USA, 20 July (2021).

61. Donahue, N. M., Epstein, S. A., Pandis, S. N. & Robinson, A. L. A two-dimensional volatility basis set: 1. Organic-aerosol mixing thermodynamics. *Atmos. Chem. Phys.* **11**, 3303–3318 (2011).
62. May, A. A. et al. Gas-particle partitioning of primary organic aerosol emissions: 3. Biomass burning. *J. Geophys. Res.*, **118**, 11327–11338 (2013).
63. Guenther, A. et al. Estimates of global terrestrial isoprene emissions using MEGAN (Model of Emissions of Gases and Aerosols from Nature). *Atmos. Chem. Phys.* **6**, 3181–3210 (2006).
64. O'Dowd, C. D. et al. A combined organic-inorganic sea-spray source function. *Geophys. Res. Lett.* **35**, L01801 (2008).
65. Monahan, E. C.; Spiel, D. E.; Davidson, K. L. A model of marine aerosol generation via whitecaps and wave disruption. In *Oceanic Whitecaps*; Monahan, E. C., Niocaill, G. M., Eds; Springer: Dordrecht, The Netherlands, Volume 2, pp. 167–174.(1986)
66. Juginovic, A., Vukovic, M., Aranza, I. & Bilos, V. Health impacts of air pollution exposure from 1990 to 2019 in 43 European countries. *Nat. Sci. Rep.* **11**, 22516 (2021).

ACKNOWLEDGEMENTS

We acknowledge the help of Katerina Seitanidi, Dontavious Sippial, Maria Kanakidou and Kacper Blaziak with the field measurements. This research has been supported by the Hellenic Foundation for Research and Innovation (project CHEVOPIN, grant no. 1819) and the EU H2020 project "Sustainable Access to Atmospheric Research Facilities (ATMO-ACCESS)" (grant number 101008004).

AUTHOR CONTRIBUTIONS

C.N.V. and A.M. performed the field measurements. C.N.V. performed the corresponding data analysis. K.S., V.S., I.K. and D.P. performed the modeling. A.A., M.G., K.F., C.K., A.K. and E.K. contributed to the measurements and performed offline analyses in the laboratory. K.E. and S.N.P. were responsible for the measurements of metals. A.N. directed the OP measurements. S.N.P. conceived and directed the study and edited the paper. C.N.V. wrote the paper with input from all co-authors.

COMPETING INTERESTS

The authors declare no competing interests.

ADDITIONAL INFORMATION

Supplementary information The online version contains supplementary material available at <https://doi.org/10.1038/s41612-023-00544-7>.

Correspondence and requests for materials should be addressed to Spyros N. Pandis.

Reprints and permission information is available at <http://www.nature.com/reprints>

Publisher's note Springer Nature remains neutral with regard to jurisdictional claims in published maps and institutional affiliations.



Open Access This article is licensed under a Creative Commons Attribution 4.0 International License, which permits use, sharing, adaptation, distribution and reproduction in any medium or format, as long as you give appropriate credit to the original author(s) and the source, provide a link to the Creative Commons license, and indicate if changes were made. The images or other third party material in this article are included in the article's Creative Commons license, unless indicated otherwise in a credit line to the material. If material is not included in the article's Creative Commons license and your intended use is not permitted by statutory regulation or exceeds the permitted use, you will need to obtain permission directly from the copyright holder. To view a copy of this license, visit <http://creativecommons.org/licenses/by/4.0/>.

© The Author(s) 2023